Supplementary Information (SI) for Physical Chemistry Chemical Physics.

Supporting Information for

A facile and High-efficiency Additive Strategy Enables High-performance Aqueous Zinc-ion Batteries

Kai Yang[1]*, Jiuzhou Yu[1], Xu Zhang[1], Shaoting Wang[1], Qiang Wang[1], Ci Gao[1], Yiyao Song[1] and Xingxing Guo[1]

[1] State Grid New Energy Cloud Technology Co., Ltd., Beijing,100077, China

E-mail: Ninejoe_1st@163.com

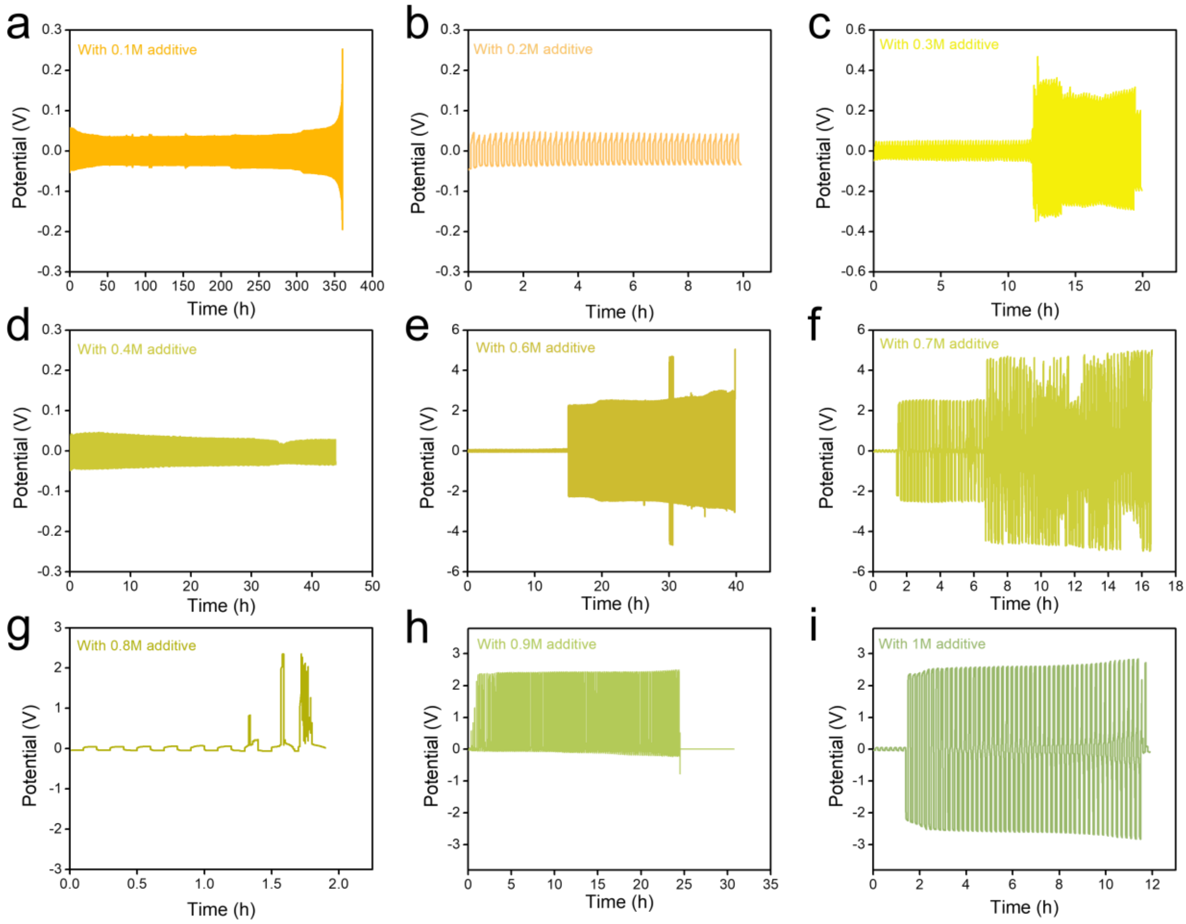

Figure S1. Cycling performance of Zn||Zn cells in 2M $ZnSO_4$ electrolyte with (a) 0.1M, (b) 0.2M, (c) 0.3M, (d) 0.4M, (e) 0.6M, (f) 0.7M, (g) 0.8M, (h) 0.9M, (i) 1M AS additive with a current density of 0.5 mA cm^{-2} and an areal capacity of 0.05 mAh cm^{-2}.

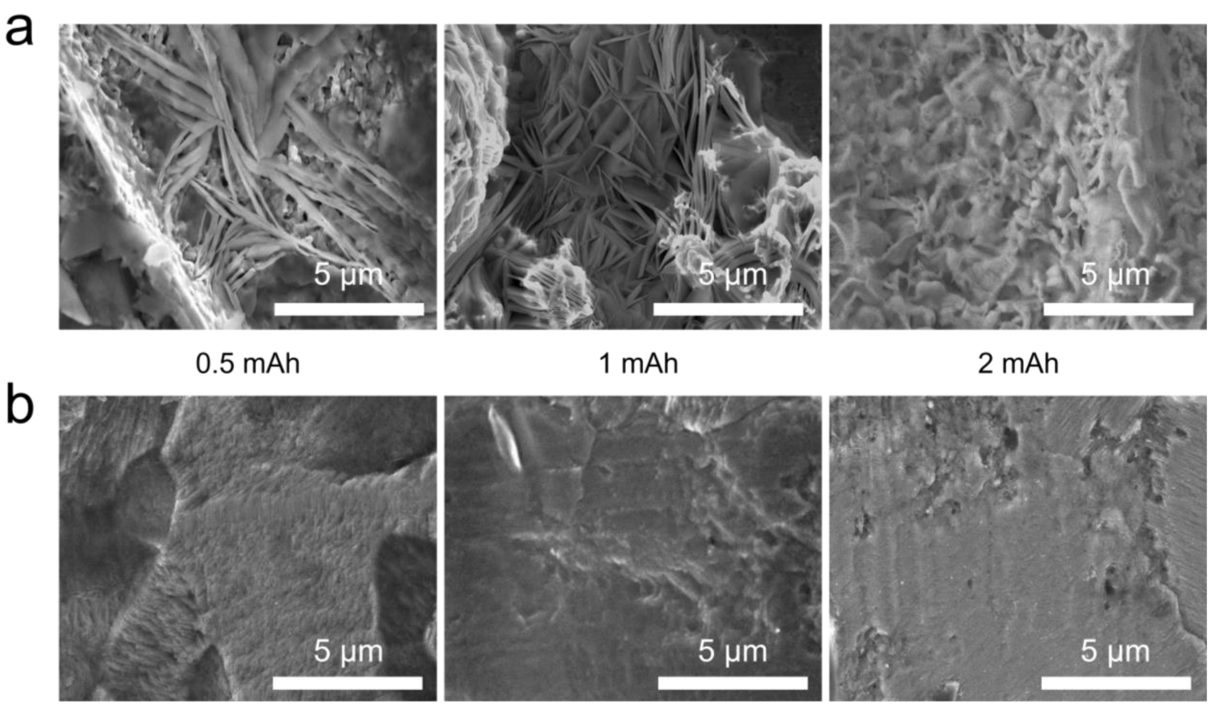

Figure S2. SEM images of ex-situ optical microscope observation of the Zn deposition process in (a) 2M $ZnSO_4$ electrolyte and (b) 2M $ZnSO_4$ electrolyte with the AS additive at the areal density of 0.5, 1, and 2 mAh cm–2.

Figure S3. The in-situ optical observation experimental setup.

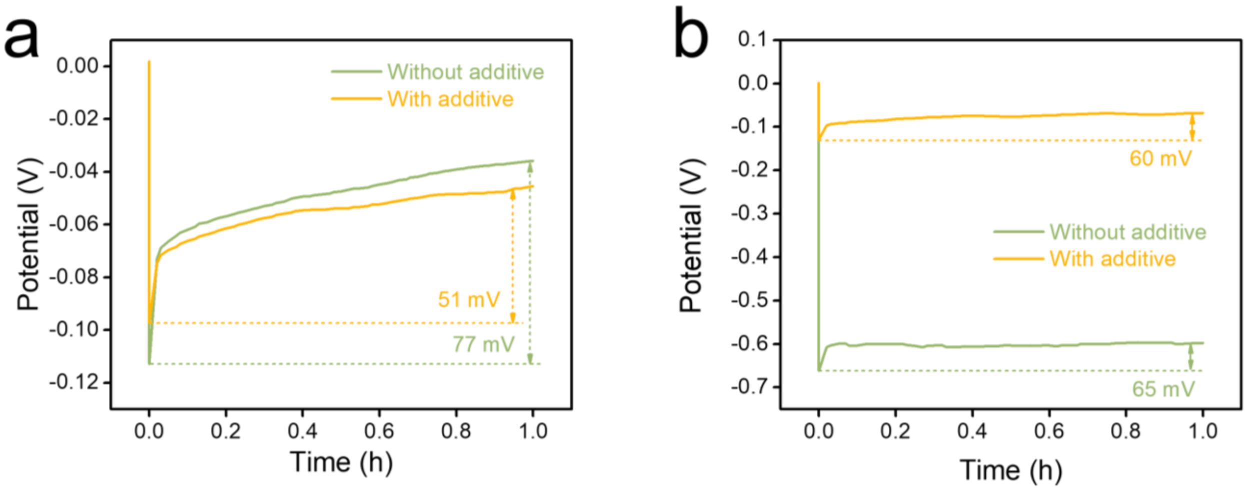

Figure S4. Voltage profiles of galvanostatic Zn deposition on Zn anode at a current density of (a) 2 mA cm^{-2} and (b) 5 mA cm^{-2}.

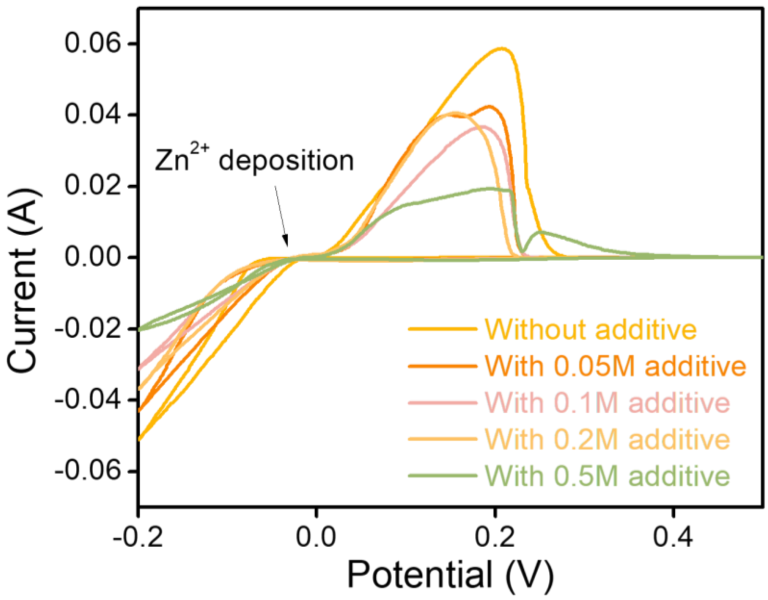

Figure S5. CV curves of Zn||Cu batteries in both 2M $ZnSO_4$ and 2M $ZnSO_4$ with 0.1M, 0.2M, 0.5M AS additive, respectively.

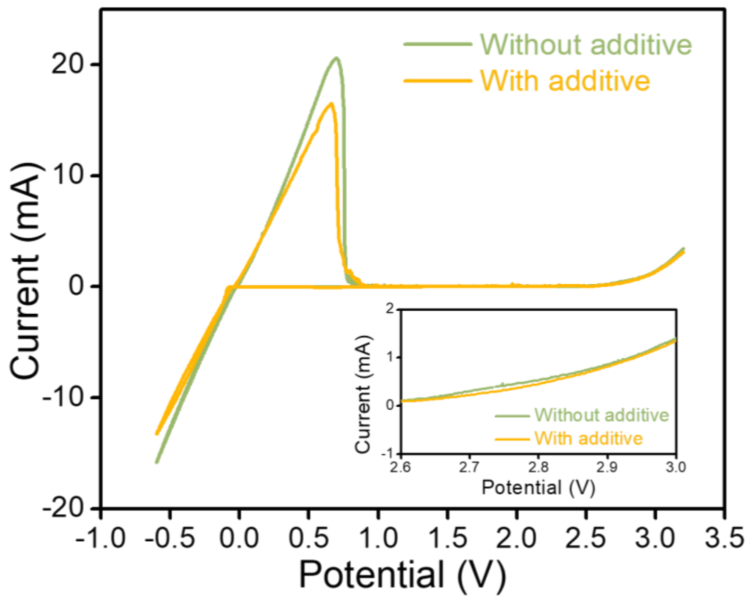

Figure S6. The electrochemical windows of 2M $ZnSO_4$ electrolyte and 2M $ZnSO_4$ electrolyte with the AS additive by three-electrode system. Working electrode: Pt. Reference and counter electrode: pristine Zn.

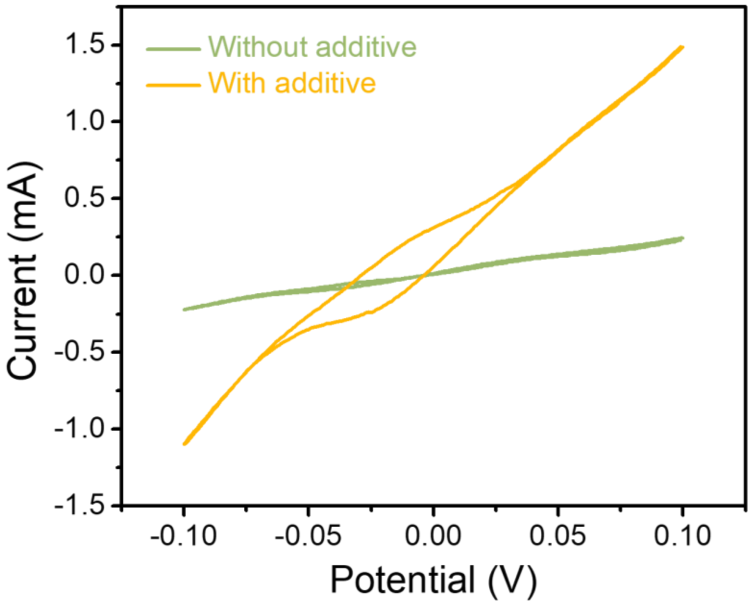

Figure S7. CV curves of Zn||Zn coin cells at a scan rate of 1mV s^{-1}.

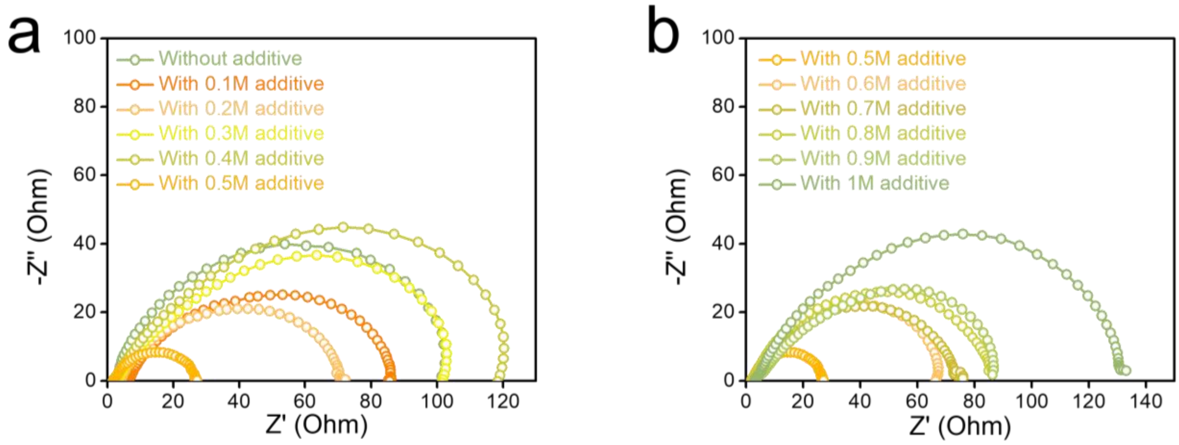

Figure S8. EIS plots of Zn||Zn batteries in (a) 2M $ZnSO_4$ electrolyte with 0M, 0.1M, 0.2M, 0.3M, 0.4M and 0.5M additive and (b) 0.5M, 0.6M, 0.7M, 0.8M, 0.9M, 1M AS additive.

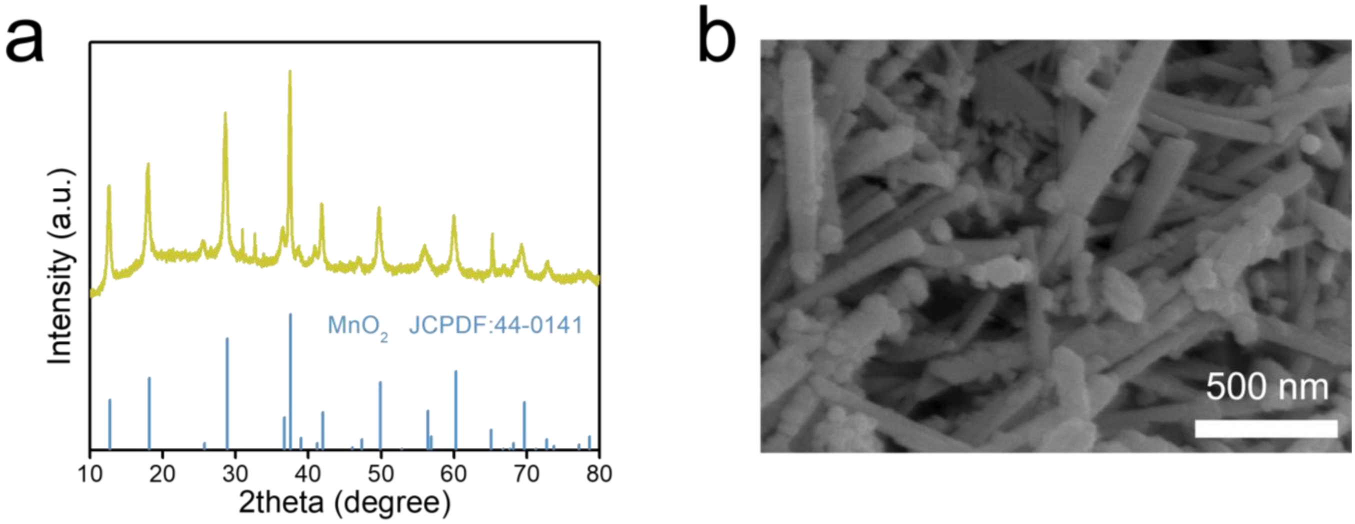

Figure S9. (a) XRD pattern and (b) SEM images of MnO_2 nanosheets cathode.

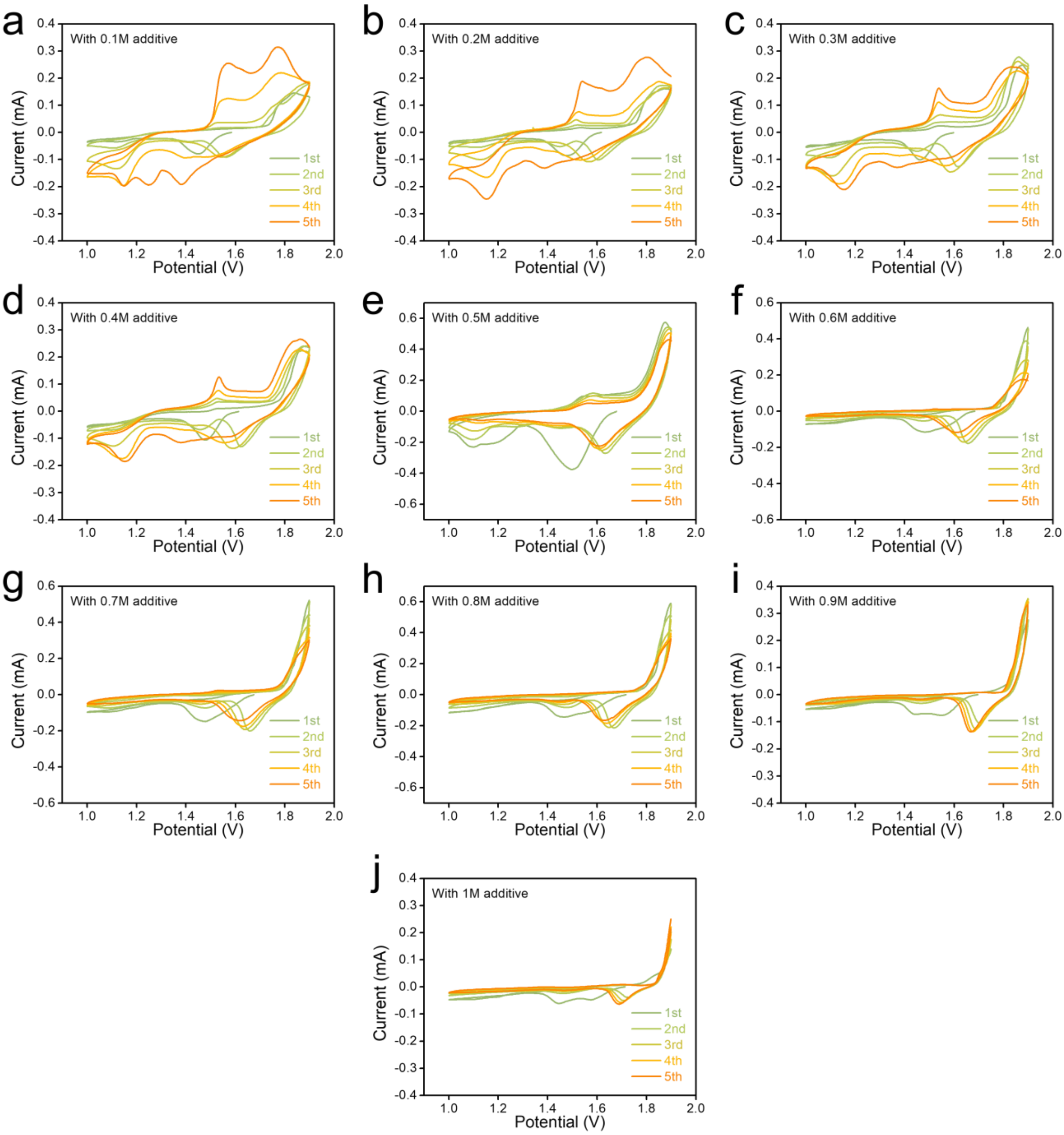

Figure S10. CV tests of Zn||MnO_2 full cells in 2M $ZnSO_4$ electrolyte with (a) 0.1M, (b) 0.2M, (c) 0.3M, (d) 0.4M, (e) 0.5M, (f) 0.6M, (g) 0.7M, (h) 0.8M, (i) 0.9M (j) 1M AS additive, respectively.

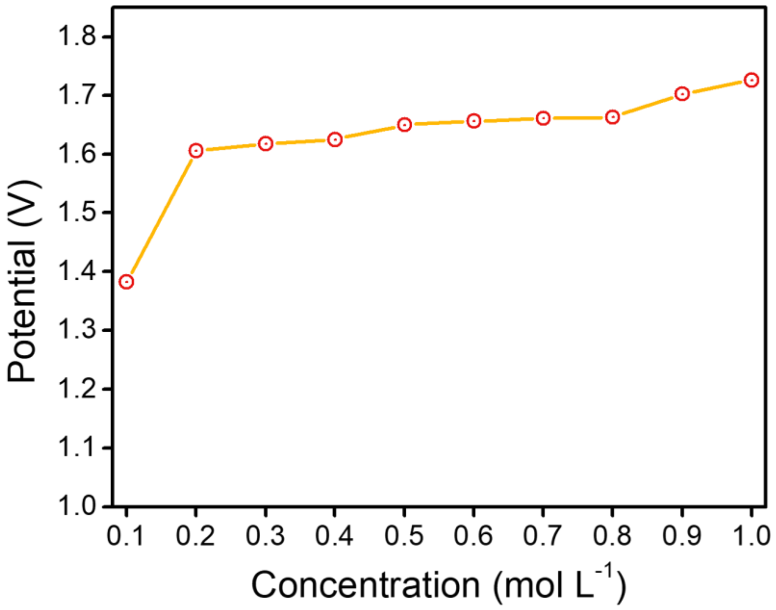

Figure S11. The potential of cathodic peak at 2nd cycle of CV tests versus additive concentration curve.

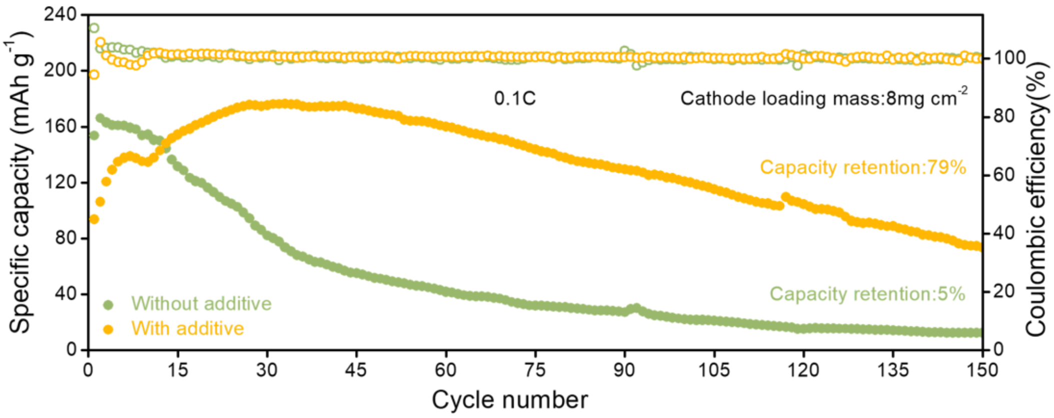

Figure S12. Long-term cycling stability with the corresponding Coulombic efficiency of coin cells in 2M $ZnSO_4$ electrolyte with the AS additive at 0.1C (1C=308 mAh g^{-1}), with 8 mg cm^{-2} cathode loading mass.

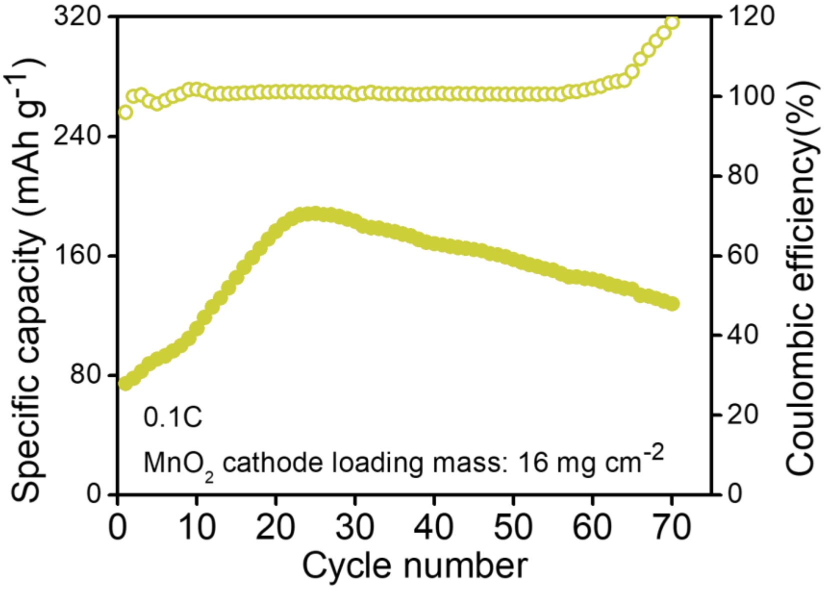

Figure S13. Long-term cycling stability with the corresponding Coulombic efficiency of coin cells in 2M $ZnSO_4$ electrolyte with the AS additive at 0.1 C (1 C = 308 mAh g^{-1}), with 16 mg cm^{-2} cathode loading mass.

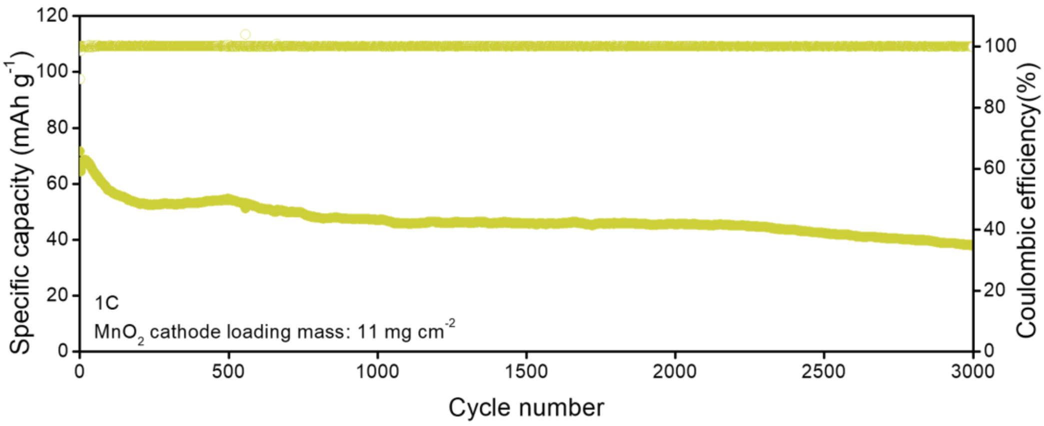

Figure S14. Long-term cycling stability with the corresponding Coulombic efficiency of coin cells in AS electrolyte at 1C (1C=308mAh g^{-1}), with 11 mg cm^{-2} cathode loading mass.

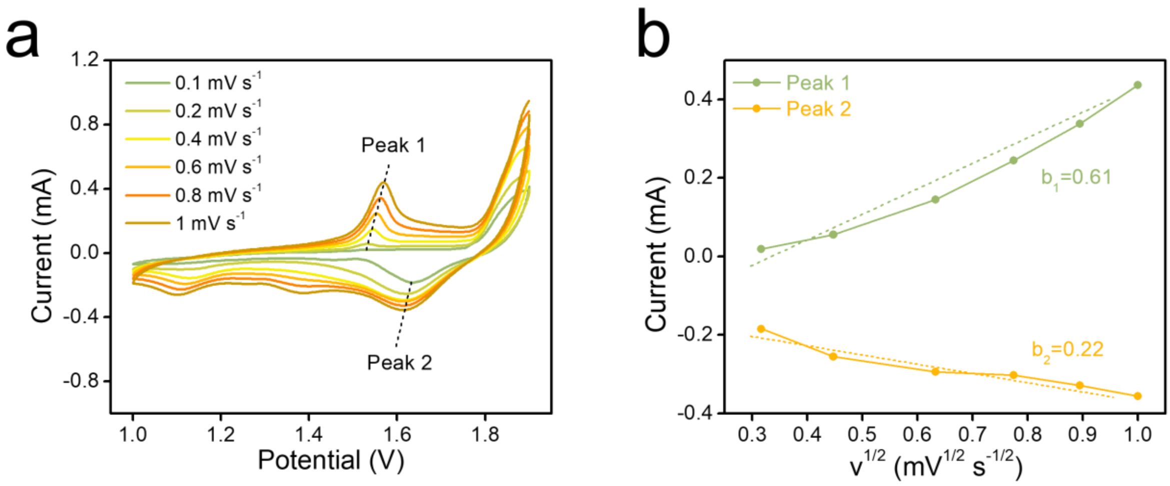

Figure S15. Kinetic analysis of the electrochemical reactions in MnO_2 electrode. (a) CV curves of Zn||MnO_2 battery in 2M $ZnSO_4$ electrolyte with the AS additive at different scan rates. (b) ***b*** value determination at the peak. according to the following equation:

The peak current (*i*) of CVs is assumed to obey a dependency of the sweep rate (*v*) as follows:

$$i = av^b$$

which could be rewritten as

$\log i = b \log v + \log a$

where ***b*** represents the slope of log(*i*) *vs.* log(*v*) curve. As for the value approaches to 0.5, the charge storage in electrode material is controlled by solid-state diffusion of active ions, whereas the ion migration is controlled by the electrochemical capacitive process when it is close to 1.

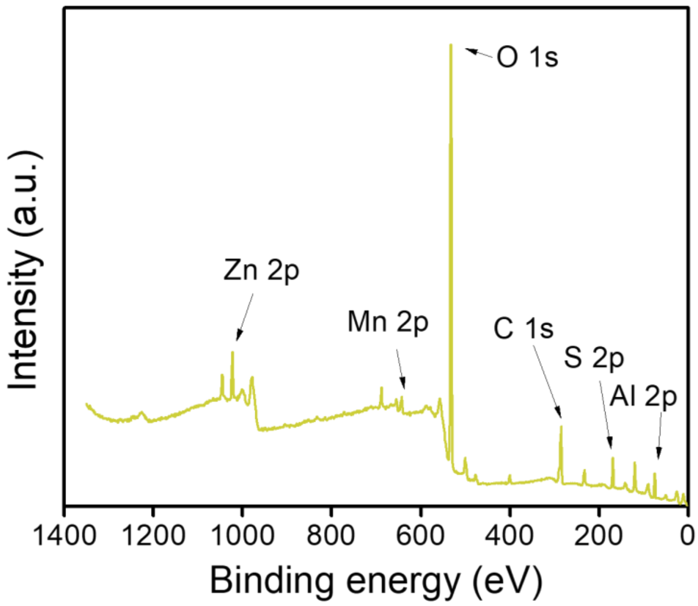

Figure S16. XPS spectra of MnO_2 cathode after 30 cycles in 2M $ZnSO_4$ electrolyte with a AS additive.

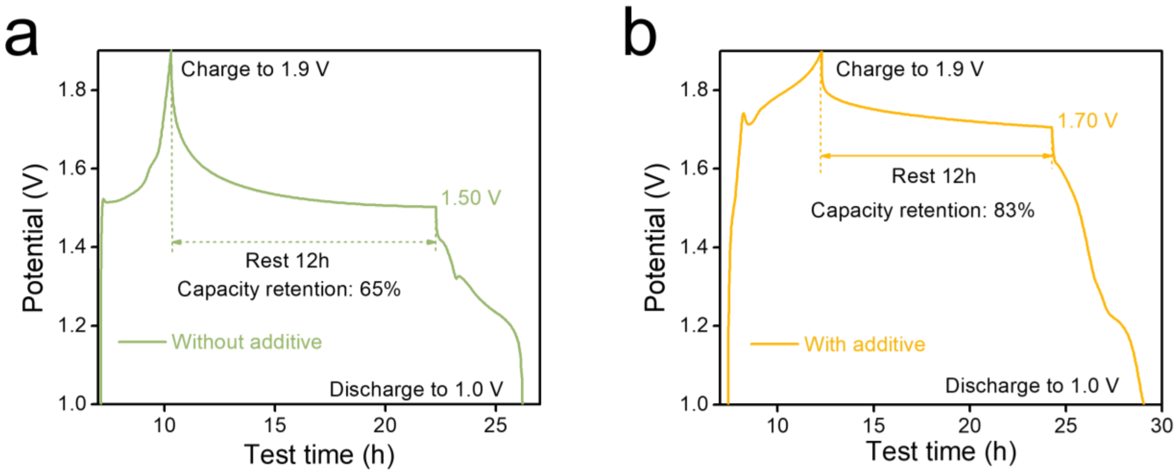

Figure S17. Storage performance of the Zn||MnO_2 coin cells in (a) 2M $ZnSO_4$ electrolyte and (b) 2M $ZnSO_4$ electrolyte with the AS additive, respectively.

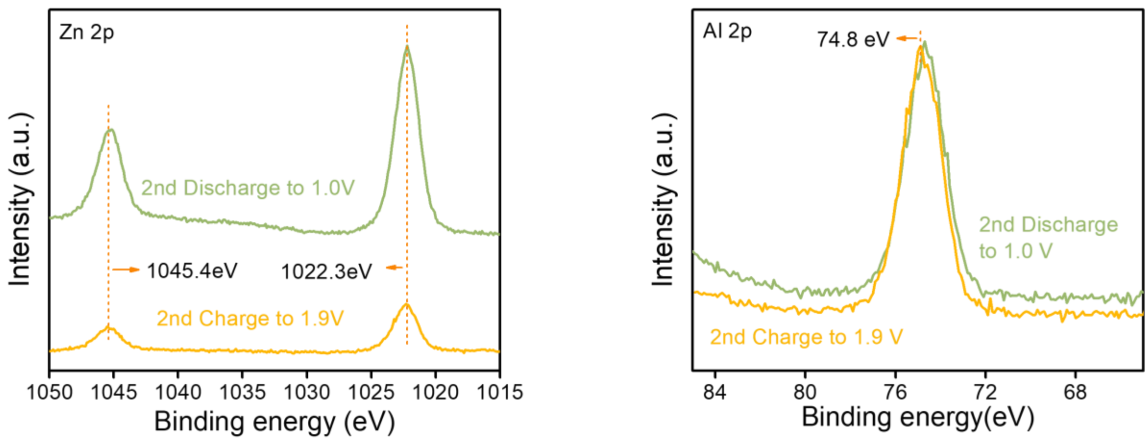

Figure S18. The ex-situ XPS spectra of (a)Zn 2p and (b)Al 2p for MnO_2 electrode after the second cycle at different states.

Table S1 The cost comparison of $ZnSO_4$ and $Al_2(SO_4)_3$ and other common salts and additives for aqueous electrolytes of zinc-ion batteries (Note: the prices are based on the same pack size of 500g, obtained from aladdin).

Zinc salt/Additive	**Price ($)**
$ZnSO_4 \cdot 7H_2O$	6.65
$Zn(CF_3SO_3)_2$	183.29
$ZnCl_2$	83.17
$ZnBr_2$	37.75
$Al_2(SO_4)_3 \cdot 18H_2O$	8.32
$MnSO_4 \cdot H_2O$	27.76
$NiSO_4 \cdot 6H_2O$	14.56
$CoSO_4 \cdot 7H_2O$	24.42
$CuSO_4 \cdot 5H_2O$	9.7
$PbSO_4$	24.94
$C_6H_7O_6Na$	26.51
Propylene glycol (PG)	17.9
Tripropylene glycol (TG)	12.48
Nitrilotriacetic acid (NTA)	7.35
N, N-dimethyl acetamide (DMA)	9.71
Citric acid	18.45
CTAB	21.64

Table S2 Fitting results of the corrosion potential and corrosion current density of Zn anode using ZS or AS electrolyte.

Electrolytes	Corrosion potential (V)	Corrosion current (mA cm^{-2})
2M $ZnSO_4$	1.026	3.101
2M $ZnSO_4$+0.5M $Al_2(SO_4)_3$	0.961	2.573

Table S3 Fitting results of the EIS of the Zn||Zn cells using pure ZS or AS electrolyte.

Electrolytes	$R_s(\Omega)$	$R_{ct}(\Omega)$
2M $ZnSO_4$	13.39	102.10
2M $ZnSO_4$+0.5M $Al_2(SO_4)_3$	3.17	27.22

Table S4 Summary of the electrochemical performance of manganese oxides-based with different electrolytes in recent researches of aqueous ZIBs.

Cathode materials	Electrolytes	Loading mass of the cathode ($mg\ cm^{-2}$)	Long cycling stability	Ref.
α-MnO_2	$2MZnSO_4$+$0.5MAl_2(SO_4)_3$	8.0 2.96	78%,1200cycles,1C 88.9%,1600cycles,1C	This work
$Na_{0.44}MnO_2$	$1MZnSO_4$+$1MNa_2SO_4$+ $0.1MMnSO_4$+0.01MSDS	1.5	93%,1500cycles,1C	[1]
$Na_{0.55}Mn_2O_4{\cdot}1.5H_2O$	$2MZnSO_4$+$0.5MNa_2SO_4$+ $0.1MMnSO_4$	1~2	93%,10000 cycles,6.5C	[2]
α-MnO_2	$1MZn(CF_3SO_3)_2$+$1MAl(CF_3SO_3)_3$	2	99.4%,1000cycles,1C	[3]
$K_{0.14}MnO_{1.96}$	$2MZnSO_4$+6%volNMP	2	95.96%,2000cycles,1 A g^{-1}	[4]
O_d-MnO_2	$1MZnSO_4$+$0.2MMnSO_4$	1	84%,2000cycles,5A g^{-1}	[5]
MnO_2	$1M(NH_4)_2SO_4$+$0.1MMnSO_4$	1	93.3%,4000cycles,4A g^{-1}	[6]
MnO_2	$2MZnSO_4$+0.5mMTMAOAc +0.025MZn(OAc)2	3.5	~77%,100cycles,0.2A g^{-1}	[7]
MnO_2	PVA/PANI/SiO_2 conductive hydrogel electrolytes	1.5~2	~77.24%,100cycles,0.2C	[8]

Table S5 DFT calculations of electrolyte structural feature and the binding energy of cations.

Cations and ligands	**Optimized structure**	**Binding Energy ($kcal\ mol^{-1}$)**
Zn^{2+} + H_2O	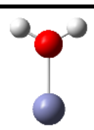	-92.8
Zn^{2+} + $2H_2O$	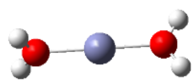	-169.5
Zn^{2+} + $3H_2O$	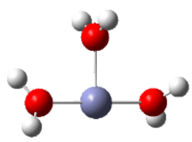	-219.3
Zn^{2+} + $4H_2O$	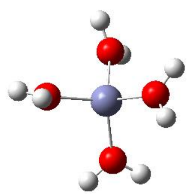	-257.4

Zn^{2+} + 5H_2O	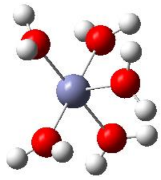	-278.0
Zn^{2+} + 6H_2O	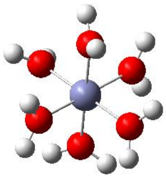	-297.7
Al^{3+} + H_2O	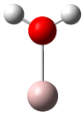	-185.3
Al^{3+} + 2H_2O	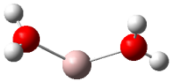	-336.7
Al^{3+} + 3H_2O	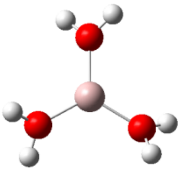	-449.6
Al^{3+} + 4H_2O	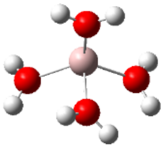	-535.9
Al^{3+}+ 5H_2O		-584.0
Al^{3+} + 6H_2O		-628.6
Zn^{2+} + SO_4^{2-}	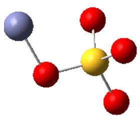	-608.9
Al^{3+} + SO_4^{2-}	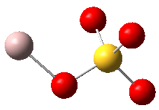	-1041.0

References:

[1] Guo, H.; Shao, Z.; Zhang, Y.; Cui, X.; Mao, L.; Cheng, S.; Ma, M.; Lan, W.; Su, Q.; Xie, E. Electrolyte additives inhibit the surface reaction of aqueous sodium/zinc battery. *Journal of Colloid and Interface Science* **2022**, *608*, 1481-1488.

[2] Xu, Y.; Zhu, J.; Feng, J.; Wang, Y.; Wu, X.; Ma, P.; Zhang, X.; Wang, G.; Yan, X. A rechargeable aqueous zinc/sodium manganese oxides battery with robust performance enabled by Na_2SO_4 electrolyte additive. *Energy Storage Materials* **2021**, *38*, 299-308.

[3] Li, N.; Li, G.; Li, C.; Yang, H.; Qin G.; Sun, X.; Li, F.; Cheng, H. Bi-Cation Electrolyte for a 1.7 V Aqueous Zn Ion Battery. *ACS Applied Materials & Interfaces* **2020**, *12 (12)*, 13790-13796.

[4] Lv, W.; Meng, J.; Li, X.; Xu, C.; Yang, W.; Duan, S.; Li, Y.; Ju, X.; Yuan, R.; Tian, Y.; Wang, M.; Lyu, X.; Pan, P.; Ma, X.; Cong, Y.; Wu, Y. Boosting zinc storage in potassium-birnessite via organic-inorganic electrolyte strategy with slight N-methyl-2-pyrrolidone additive. *Energy Storage Materials* **2023**, *54*, 784-793.

[5] Xiong, T.; Yu, Z.; Wu, H.; Du, Y.; Xie, Q.; Chen, J.; Zhang, Y.; Pennycook, S.; Lee, W.; Xue, J. Defect Engineering of Oxygen-Deficient Manganese Oxide to Achieve High-Performing Aqueous Zinc Ion Battery. *Advanced Energy Materials*, **2019**, *9 (14)*, 1803815.

[6] Wang, S.; Yuan, Z.; Zhang, X.; Bi, S.; Zhou, Z.; Tian, J.; Zhang, Q.; Niu, Z. Non-Metal Ion Co-Insertion Chemistry in Aqueous Zn/MnO2 Batteries. *Angewandte Chemie International Edition*, **2021**, *133 (13)*, 7132-7136.

[7] Li, L.; Xie, Y. H.; Yao, M. L.; Cao, R.; Mai, X. Y.; Ji, Y.; Chen, L.; Dong, X. L.; Xia, Y. Y. Dual-additive-based Electrolyte Design for Aqueous Zinc Ion Batteries with High Plating/Stripping Efficiency. *Chemical Communications* **2024**, *60 (53)*, 6809-6812.

[8] Zhu, Z.; Wang, L.; Tang, X.; Li, L.; Shi, Y.; Shao, J. Application of Poly(vinyl alcohol) Conductive Hydrogel Electrolytes in Zinc Ion Batteries. *Chinese Journal of Inorganic Chemistry* **2025**, *41 (5)*, 893-902.